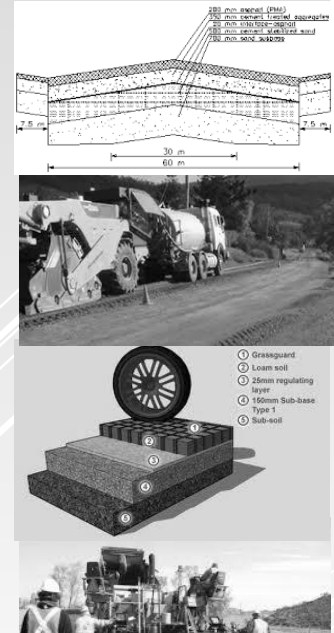


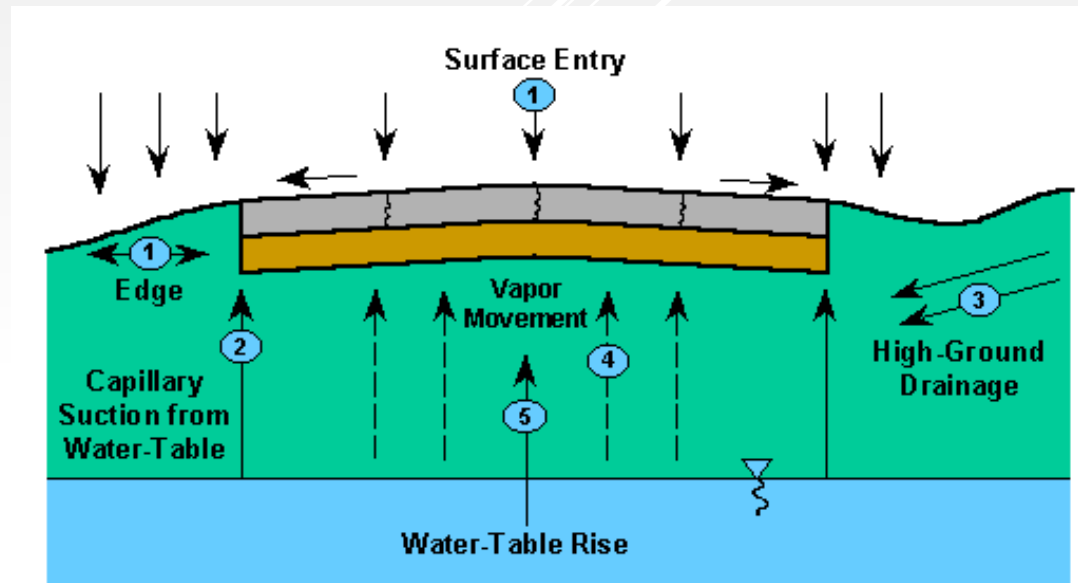
# LECTURE 7: Climatic data



## 7.1 Introduction

Temperature has a significant effect on the stiffness as well as the **fatigue** and **permanent deformation** resistance of asphalt mixtures. It is therefore quite obvious that accurate knowledge of the temperature distribution in the pavement should be available in order to allow realistic analyses of the stresses and strains in asphalt pavements to be made.

Furthermore moisture has a significant effect on the stiffness and strength characteristics of unbound materials and soils. In this chapter, information will therefore be given on how values for these important input parameters can be obtained.



## 7.2 Temperature

The temperature distribution in the pavement layers can vary significantly during the day and during the seasons of the year. Figure 63 e.g. shows the temperature distribution during a hot spring and a hot summer day. One should realize that the surface temperatures can easily be 5°C higher than the temperatures measured at 10 mm below the pavement surface.

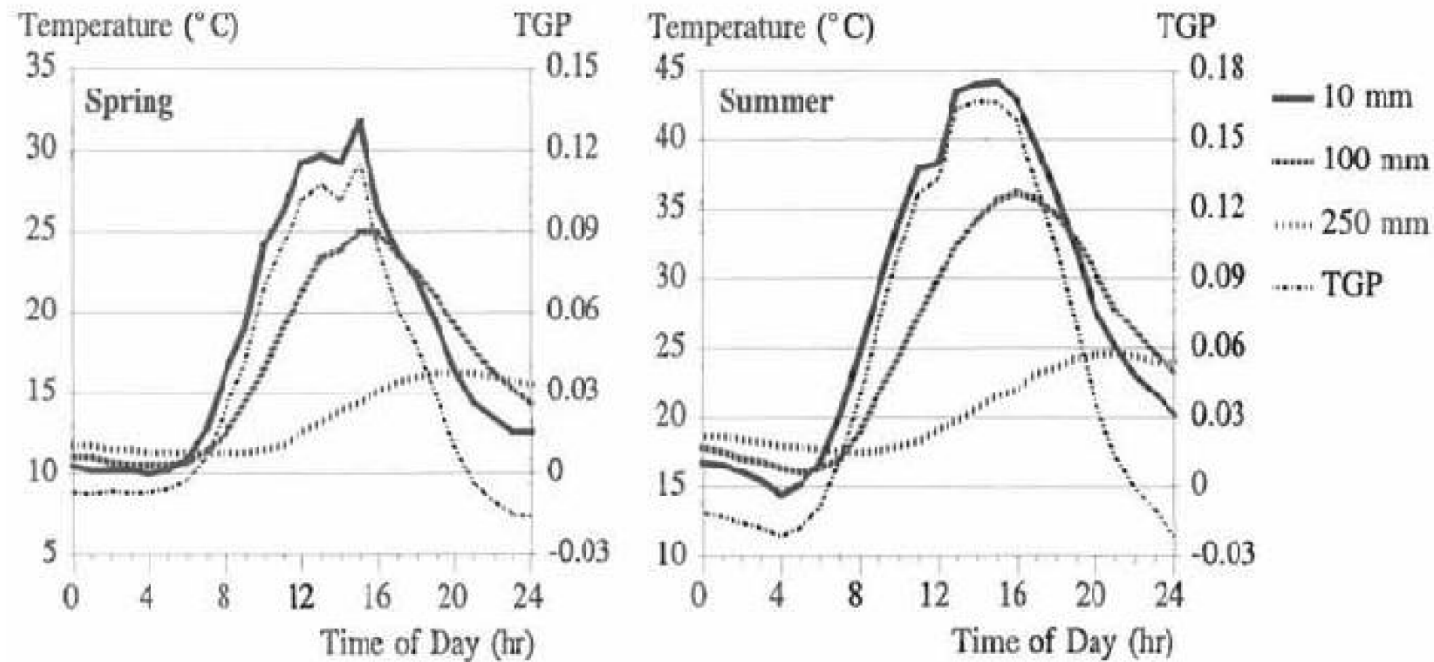


Figure 63: Temperature variations during the day over the thickness of the asphalt pavement.

Figure 64 shows the temperature gradient that exists over the asphalt layer thickness in case of the hot summer day shown in figure 63.

From these figures it is clear that assuming a constant temperature over the thickness of the asphalt layer is far from reality unless one is dealing with thin asphalt layers. Furthermore the total asphalt thickness is commonly made of different types of asphalt mixtures, especially in case the total thickness is larger than 100 mm, which implies that even when the temperature is constant over the entire thickness, different stiffness values will be found for the different layers of which the total asphalt thickness is made of.

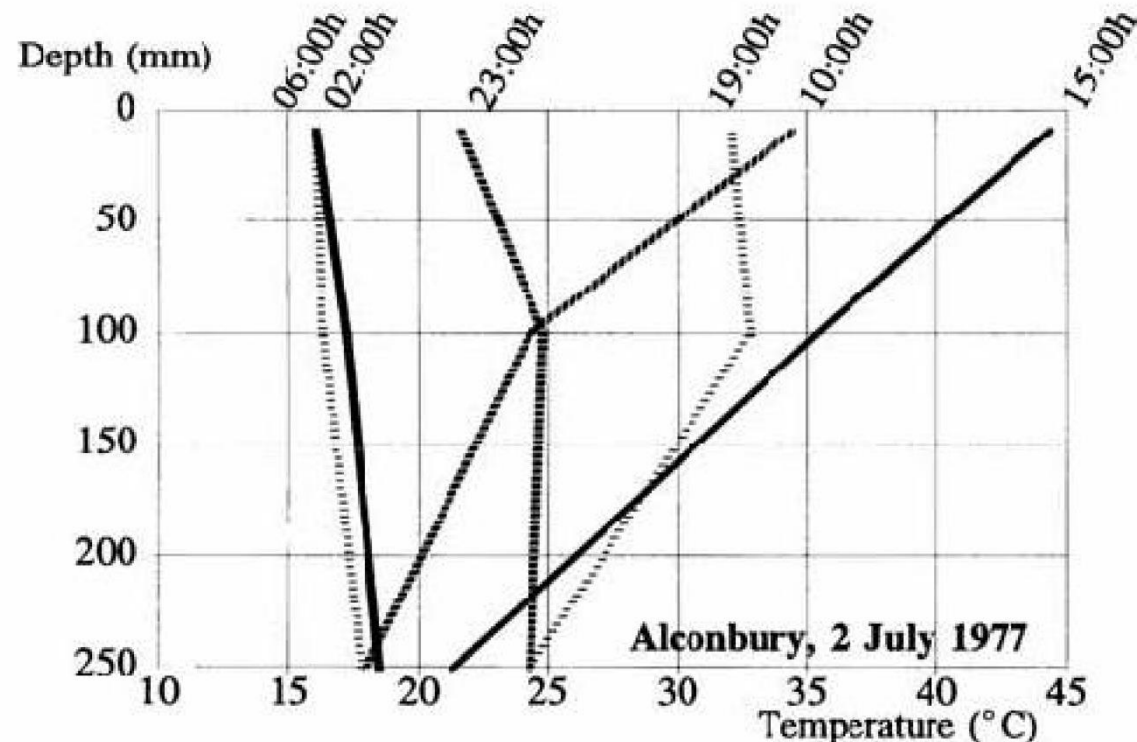


Figure 64: Temperature gradient in an asphalt pavement on a hot summer day.



Van Gurp [26] in his thesis presents a method to deal with temperature variations over the total asphalt thickness. He divided the total thickness into three sub-layers (figure 65) and defined an equivalent asphalt thickness,  $h_{1,eq}$  in the way as described in figure 66. This equivalent thickness has a modulus value equal to the modulus of the third sub-layer.

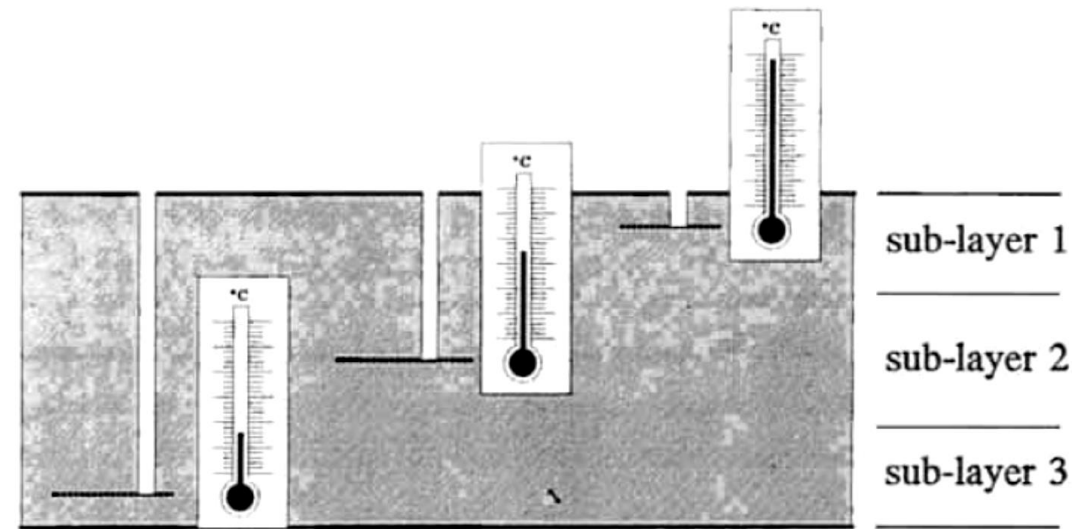


Figure 65: Dividing the total asphalt thickness in sub-layers.

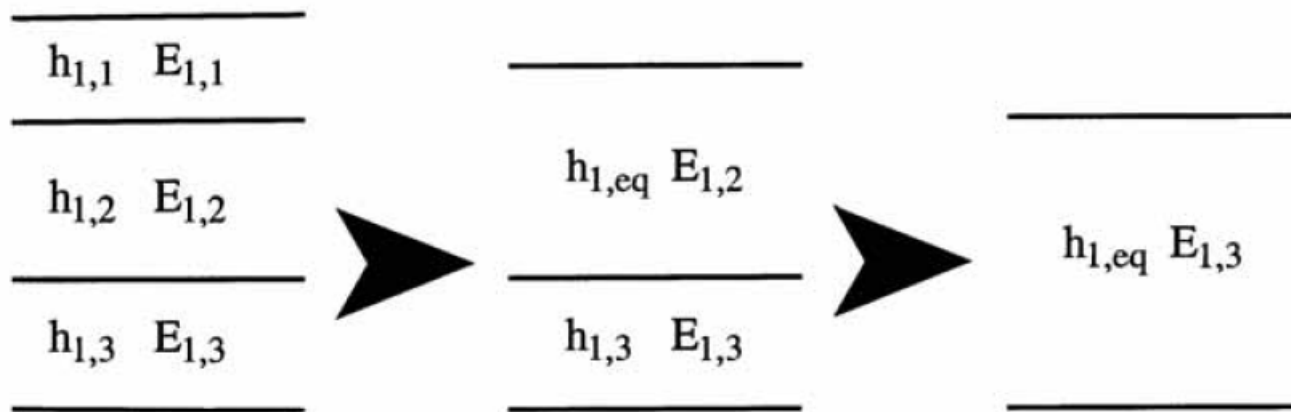


Figure 66: Calculation of the equivalent asphalt thickness  $h_{1,eq}$ .

The equivalent asphalt thickness is calculated as follows.

$$h_{1,eq} = (h_1 / 4) * [(n_1^2 n_2^2 + 64 n_1 n_2^2 + 110 n_1 n_2 + 16 n_2^2 + 64 n_2 + 1) / (n_1 n_2 + 2 n_2 + 1)]^{0.33}$$

Where:

$h_{1,eq}$  = equivalent total asphalt thickness with stiffness  $E_{1,3}$ ,

$n_1 = E_{1,1} / E_{1,2}$ ,

$n_2 = E_{1,2} / E_{1,3}$ .

This equation is valid under the assumption that  $h_{1,1} = 1/4 h_1$  and  $h_{1,3} = 1/4 h_1$  and that the temperature is uniformly distributed over each of the sub-layers. The mean temperature of each sub-layer is used to calculate the modulus of that sublayer.

In order to be able to take into account the effects of temperature gradients, Van Gurp also defined a thermal gradient parameter (TGP) being:

$$TGP = 1 - h_{1,eq} / h_1$$

TGP takes a positive value when the top part of the total asphalt thickness is softer than the bottom part. Depending on TGP, a correction on the tensile strain calculated at the bottom of the asphalt layer, should be applied following:

$$\epsilon_{r,corr} = \epsilon_{r,uncorr} * (1 - TGP)$$

Where:

$\epsilon_{r,corr}$  = asphalt strain corrected for thermal gradients,

$\epsilon_{r,uncorr}$  = asphalt strain uncorrected for thermal gradients,

TGP = thermal gradient parameter, see figure 67.

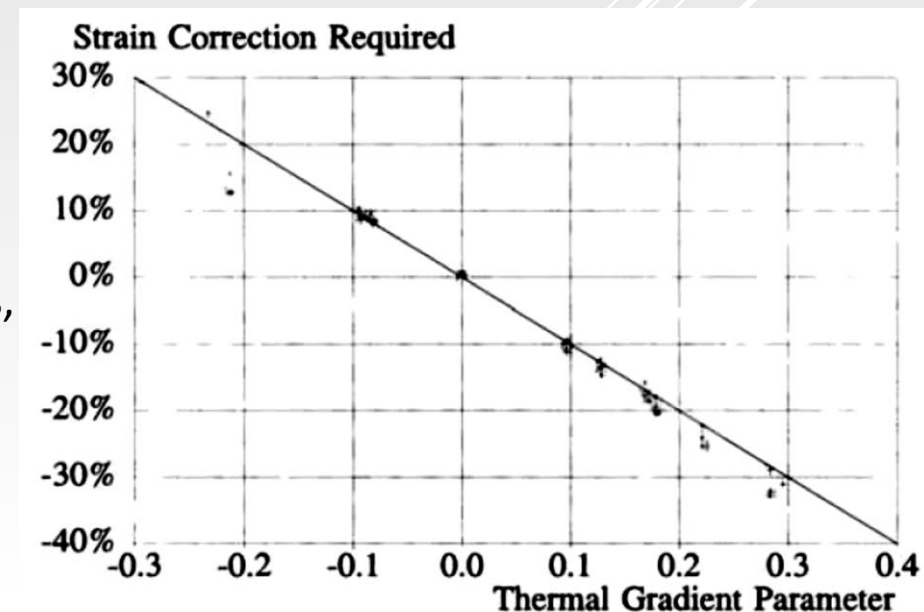


Figure 67: TGP vs strain correction required.

The procedure to use all this is as follows:

- calculate  $h_{1,eq}$ ,
- calculate the tensile strain  $\epsilon_{r,uncorr}$  at the bottom of  $h_{1,eq}$ ,
- calculate TGP,
- calculate  $\epsilon_{r,corr}$ .

Van Gurp also presented a method to predict the **asphalt temperature at a depth from the pavement surface of 1/3 of the total asphalt thickness**. This equation is:

$$T = 8.77 + 0.649 T_0 + (2.20 + 0.044 T_0) \sin \{2\pi (hr - 14) / 24\} + \log (h_1 / 100) [-0.503 T_0 + 0.786 T_5 + 4.79 \sin \{2\pi (hr - 18) / 24\}]$$

Where:

$T$  = temperature at a depth of  $1/3 h_1$  from the pavement surface,

$T_0$  = pavement surface temperature [ $^{\circ}\text{C}$ ],

$T_5$  = prior mean five days air temperature [ $^{\circ}\text{C}$ ],

$h_1$  = thickness of the asphalt layer [mm],

$hr$  = time of the day in 24 hour system.

It is clear that the determination of the temperature to be adopted in the pavement design analysis can be a rather cumbersome task especially if large variations in temperature occur during the day and during the year





. For that reason several simplification procedures have been developed and the one prepared for the Shell Pavement Design Manual [27] will be briefly described here-after.

Based on a large number of calculations, Shell researchers [28] concluded that it is possible to define a weighted mean annual air temperature (w-MAAT) such that the damage that accumulates over one year is the same as by taking into account varying temperature conditions over a year. In order to so, a weighing factor has to be determined (figure 68 and table 14) using the mean monthly air temperature (MMAT) as input. When the weighing factor is known, the weighted mean annual air temperature can be determined. The procedure is explained by means of an example.

Month	Mean monthly air temperature MMAT [ $^{\circ}\text{C}$ ]	Weighing factor from figure 68
January	8	0.21
February	8	0.21
March	12	0.36
April	16	0.62
May	19	0.93
June	22	1.40
July	26	2.35
August	28	3.00
September	22	1.40
October	19	0.93
November	12	0.36
December	6	0.16
Total of weighting factors		11.93
Average weighting factor = total / 12		$\approx 1$
Weighted mean annual air temperature w-MAAT determined from figure 68		$\approx 20^{\circ}\text{C}$

Table 14: Example how to calculate the weighted mean annual air temperature.

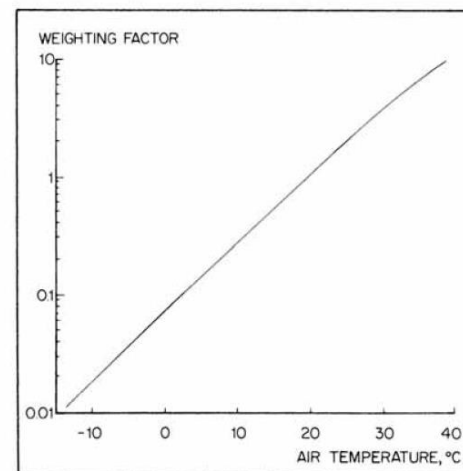


Figure 68: Temperature weighing chart.

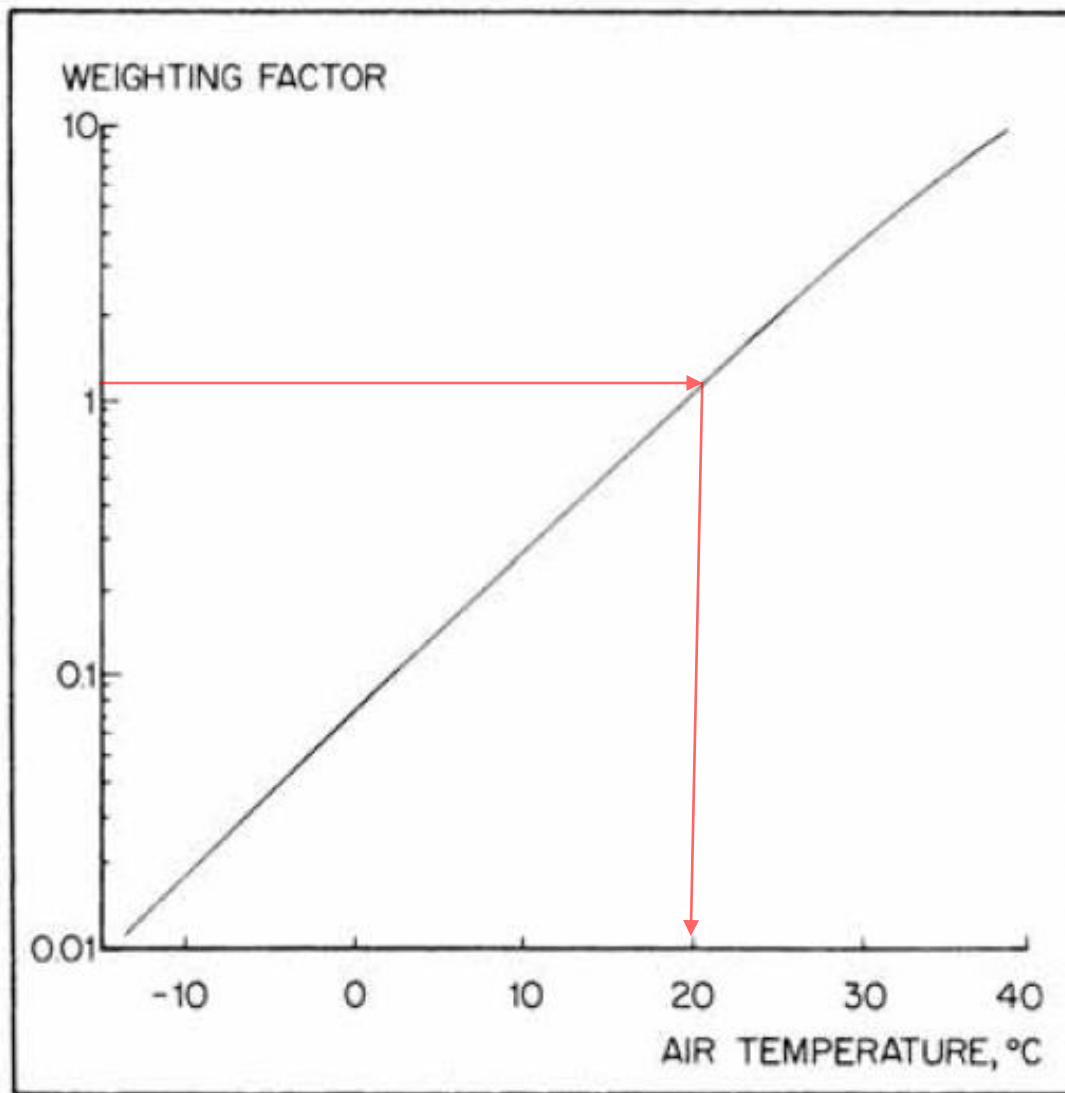


Figure 68: Temperature weighing chart.

Month	Mean monthly air temperature MMAT [ $^{\circ}\text{C}$ ]	Weighing factor from figure 68
January	8	0.21
February	8	0.21
March	12	0.36
April	16	0.62
May	19	0.93
June	22	1.40
July	26	2.35
August	28	3.00
September	22	1.40
October	19	0.93
November	12	0.36
December	6	0.16
	Total of weighting factors	11.93
	Average weighting factor = total / 12	$\approx 1$
	Weighted mean annual air temperature w-MAAT determined from figure 68	$\approx 20^{\circ}\text{C}$

Table 14: Example how to calculate the weighted mean annual air temperature.

When the weighted mean annual air temperature is known, the effective asphalt temperature is estimated using figure 69.

It should be noted that the Shell procedure described here can be used for the thickness design of asphalt pavements but not for permanent deformation analyses. In those case one should take into account the real temperature distributions.

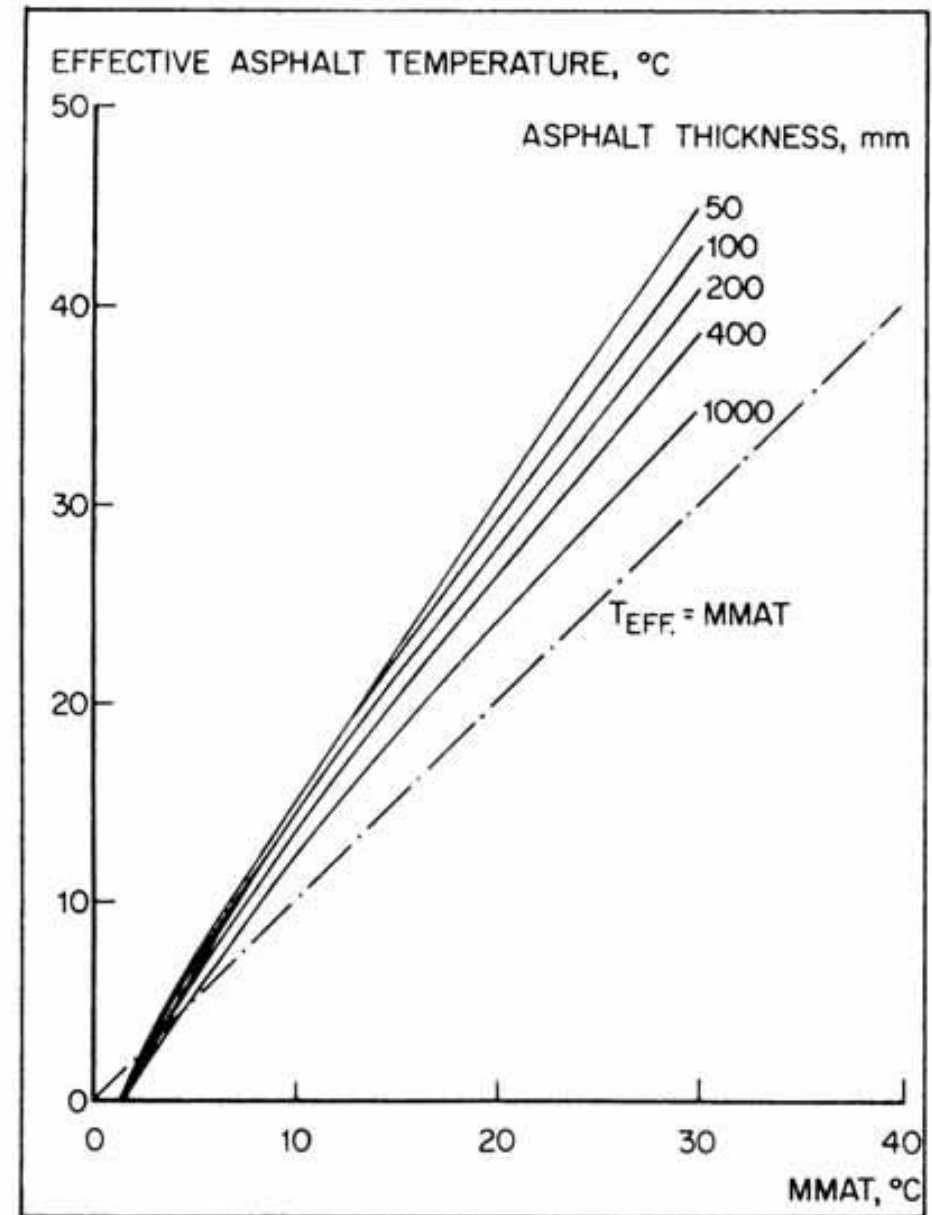
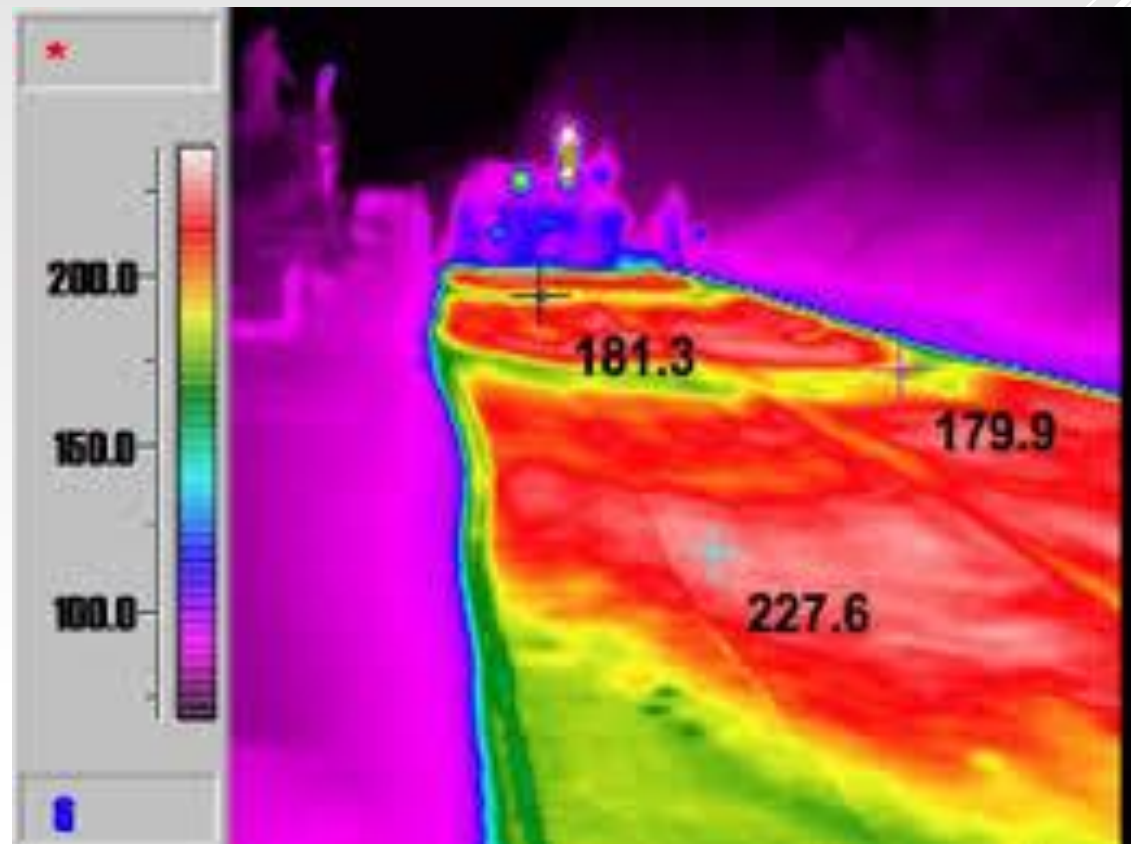


Figure 69: Effective asphalt temperature as a function of MMAT (also w-MAAT can be used) and the asphalt layer thickness.

H.W: find the effective Asphalt Temperature for Kerbala city





### 7.3 Moisture

Moisture has a large effect on the stiffness and **bearing capacity of soils** and **unbound materials** and for that reason it is important to qualify and quantify these effects. If no evaporation occurs and there are no changes in the groundwater level, the moisture conditions can be estimated from the suction characteristics of the soil. Figure 70 shows these characteristics for a number of soils.

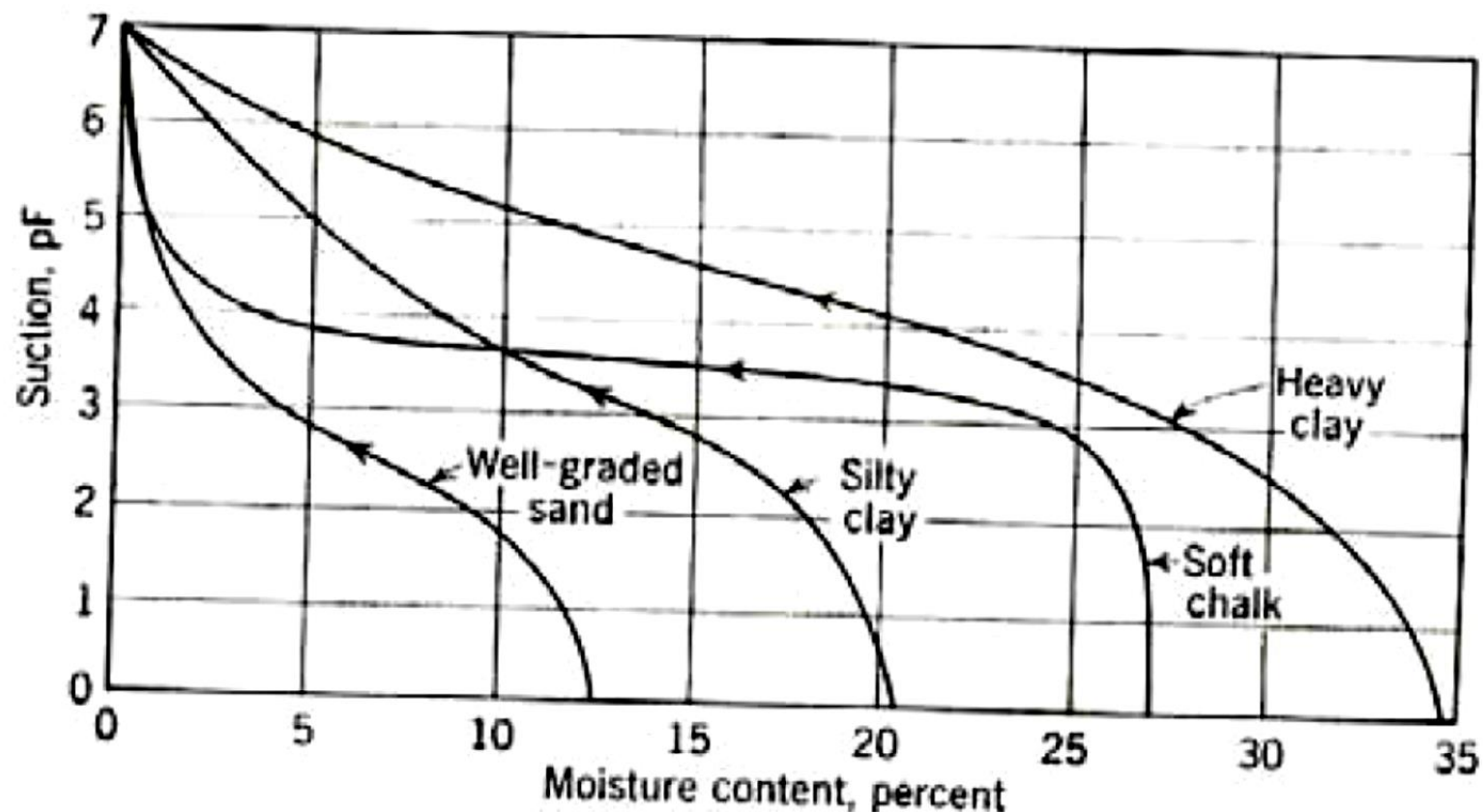


Figure 70: Suction characteristics of various soils.

In figure 70,

- the suction is given as the  $\log_{10}$  of cm of water column. This means that at a  $pF = 2$ , meaning a suction of 100 cm of water column, the moisture content in a well graded sand is about 8% while in the heavy clay it is 32%.
- One could also state that at a height of 100 cm above groundwater level the moisture content in the sand equals 8% and 32% in the clay. In this case the  $pF$  curve is used to estimate the moisture content above the groundwater level.

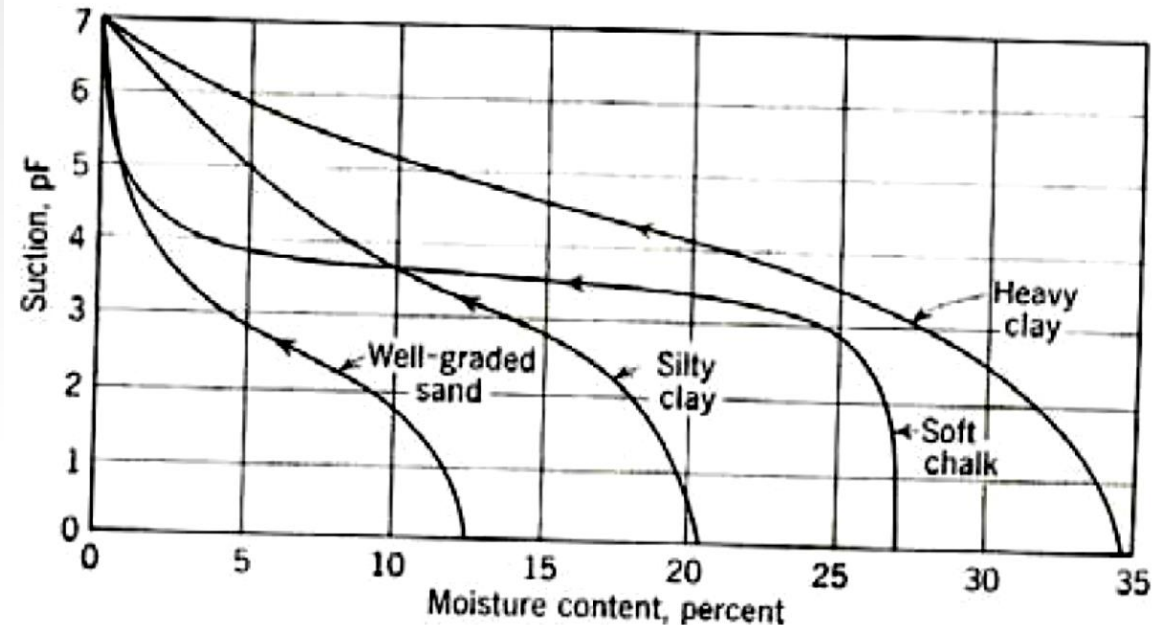


Figure 70: Suction characteristics of various soils.

- From the figure it becomes clear that if evaporation is prevented and the groundwater level is 10m below the ground level, the moisture content near the surface of a heavy clay is still 27% (10 m above groundwater level = 1000 cm above groundwater level, read the graph at  $pF = 3$ ). All this means that in this case a rather stable moisture profile develops above the groundwater level.
- In case we have a 5m thick well graded sand on top of a heavy clay and the groundwater level would be 10m below the surface, then the moisture content at the top of the sand layer would be 4% (read moisture content at  $pF = 3$ ). At 5m below the surface, the moisture content at the top of the clay would be 28% and at the bottom of the sand layer 5.5 (read  $pF$  curves at  $pF = \log 500 = 2.7$ ).

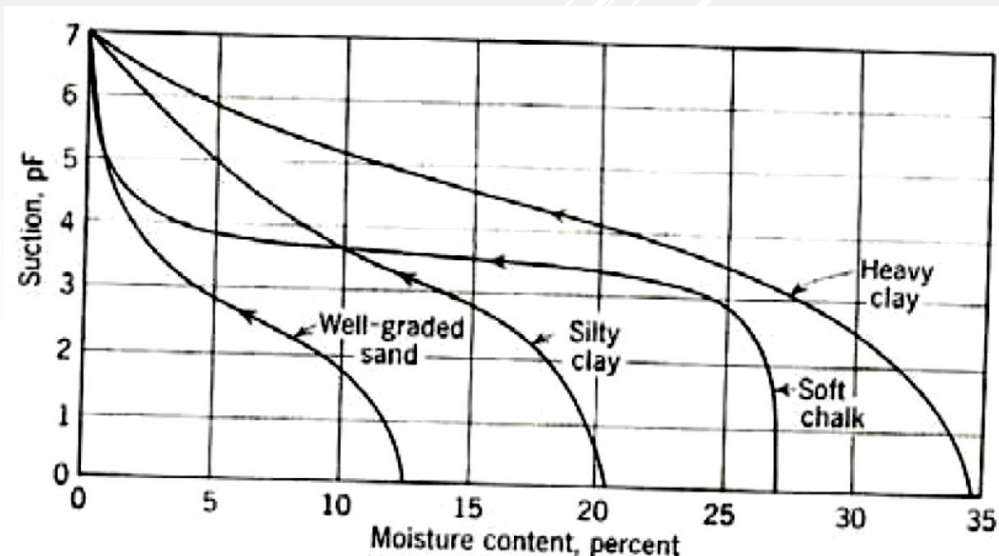


Figure 70: Suction characteristics of various soils.

Of course the moisture profile is more complex in reality because of drying or wetting of the top part of the soil. This is schematically shown in figure 71.

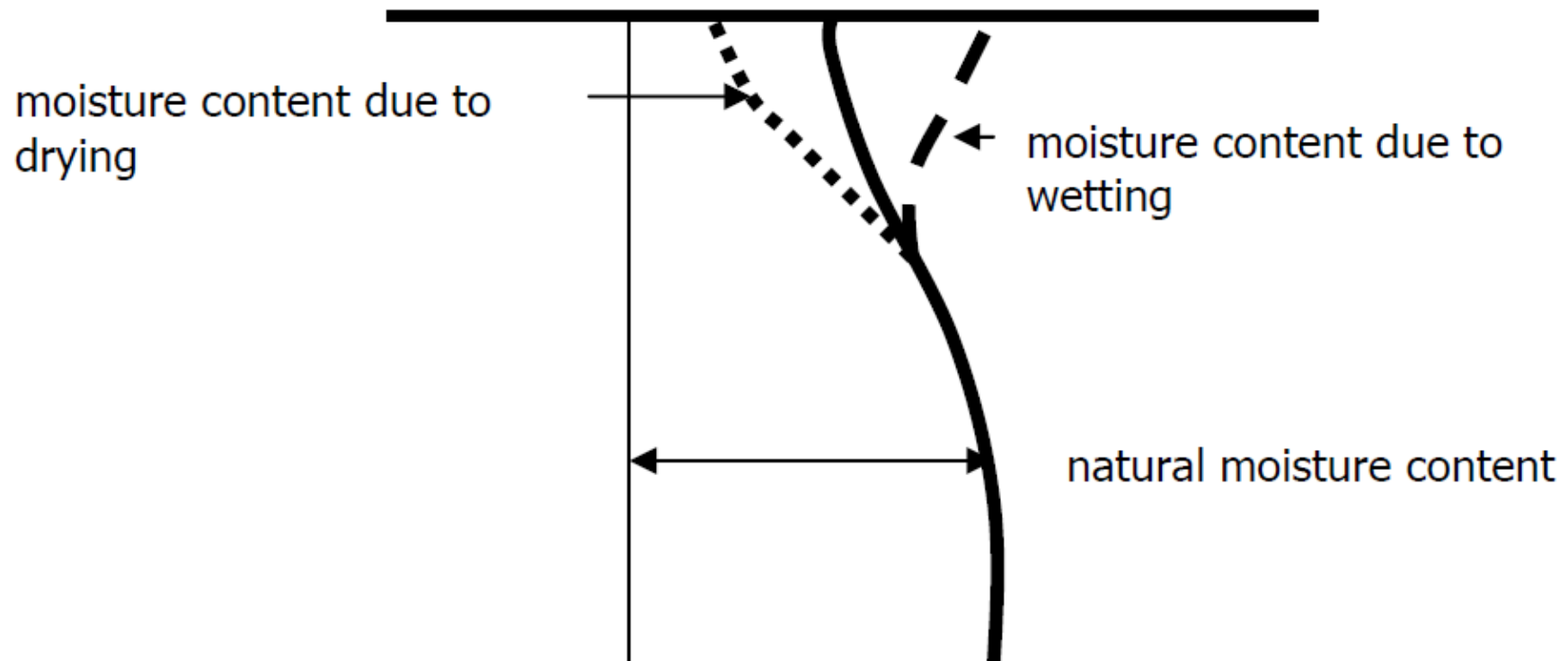


Figure 71: Moisture content variations due to drying and wetting.

Similar conditions occur in the pavement as is shown in figure 72

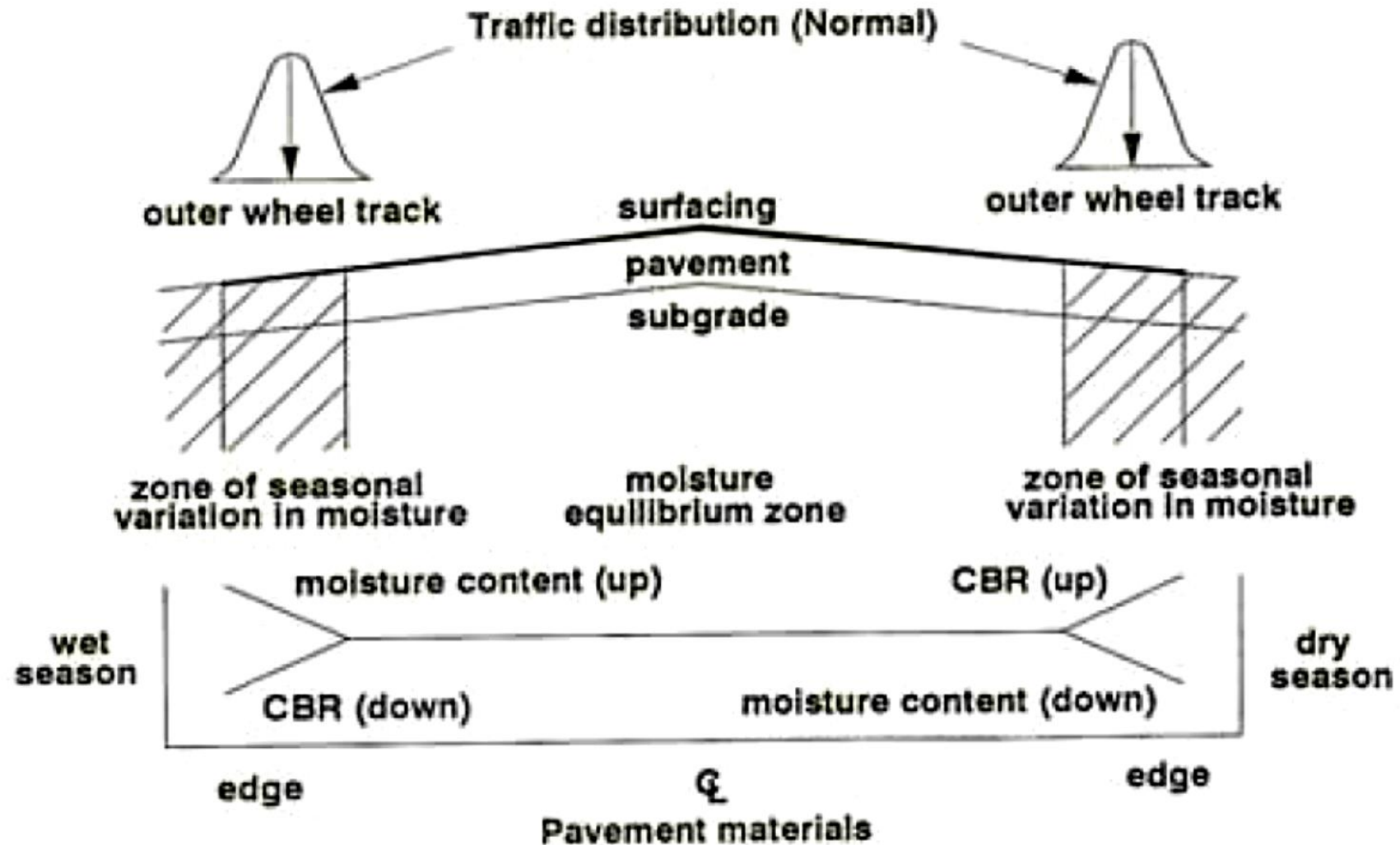


Figure 72: Variation in moisture content occur near the pavement edge.



- Figure 72 nicely shows that the zone of moisture variation, and so the zone of variation in bearing capacity and stiffness, can coincide with the area in which the outer wheels of trucks and lorries are loading the pavement. Especially during the wet period this can give rise to significant pavement problems because of the low bearing capacity of the soil at locations where the stresses due to traffic are the highest.

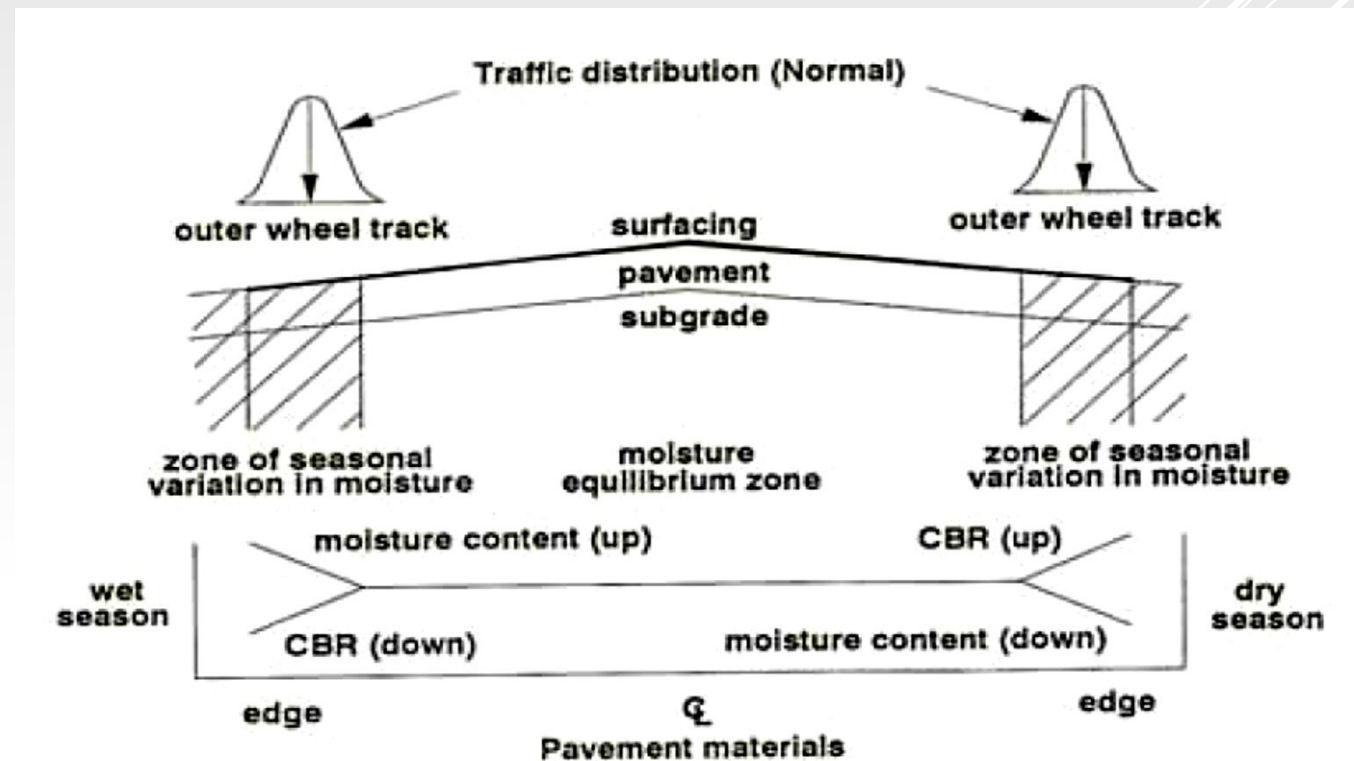


Figure 72: Variation in moisture content occur near the pavement edge

- Also in the dry season this can create problems especially when the subgrade shrinks due to moisture loss. Shrinkage near the pavement edge can result in longitudinal cracks in the pavement near the pavement edge.
- It has however been shown that moisture variations are almost negligible at a distance of approximately 1.2 m from the pavement edge. This implies that if a paved shoulder is applied having a width of 1.2 m or more, the zone that is influenced by the traffic loads doesn't coincide with the zone subjected to seasonal moisture variations.

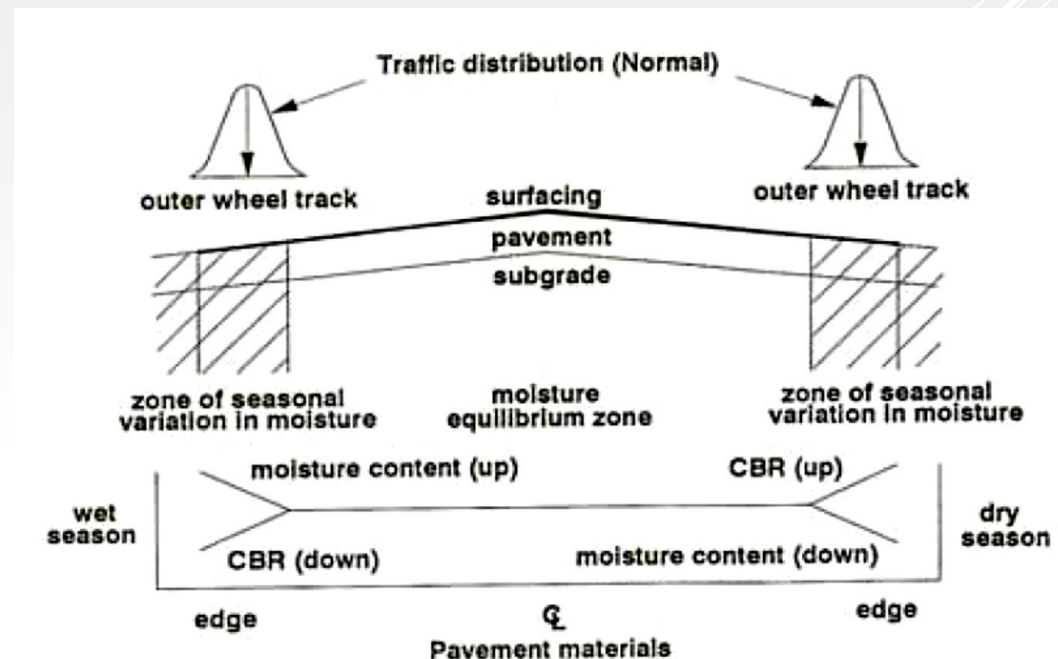


Figure 72: Variation in moisture content occur near the pavement edge.

A typical example of pavement damage that occurs due to drying of the soil is shown in figure 73. Figure 73 was made when making a study of extensive longitudinal cracking in the verge and in the pavement near the edge observed in several roads in Surinam after an extended period of draught.

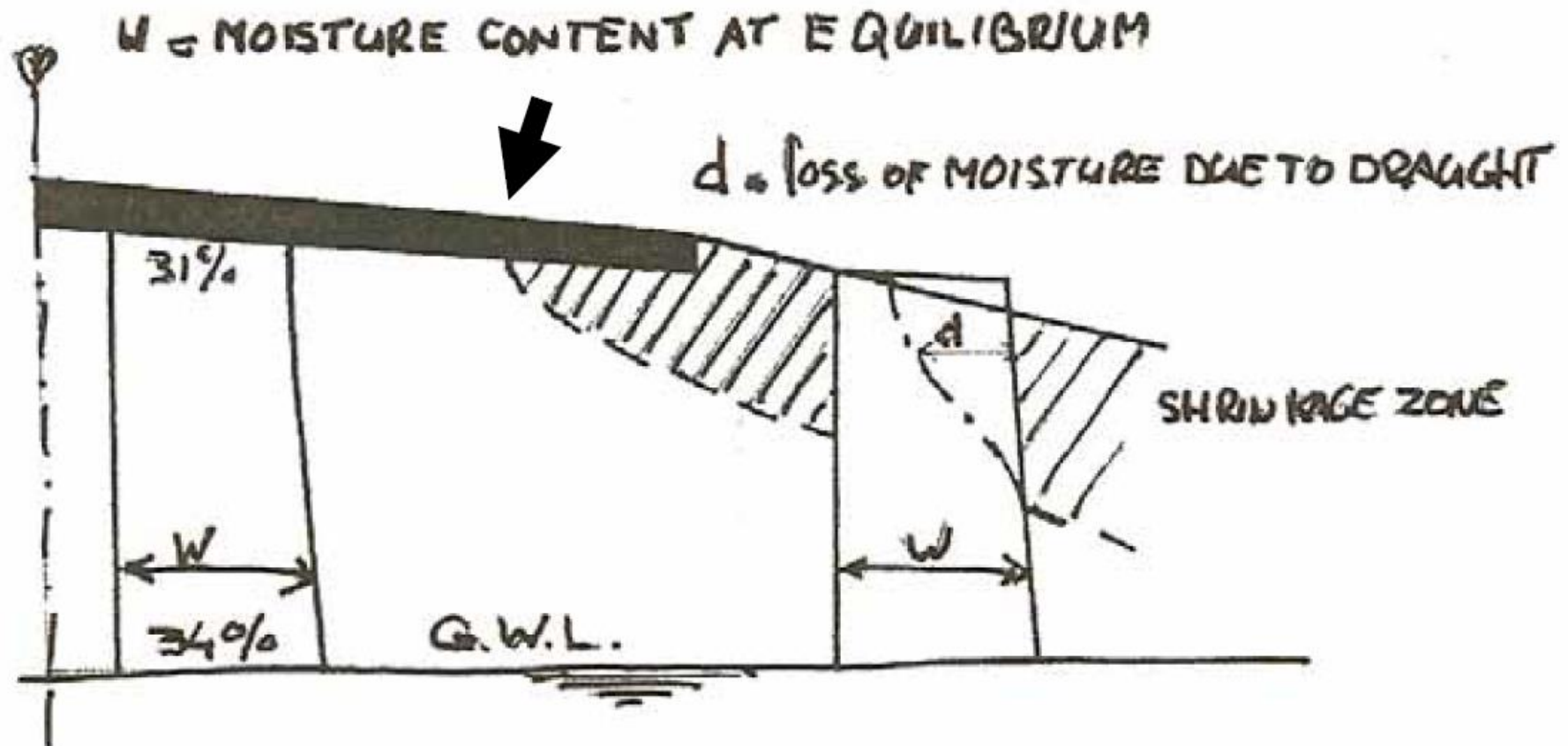


Figure 73: Due to an extended dry period, the subgrade under the pavement edge started to shrink resulting in significant cracking at location of the arrow.

Figure 74 shows the changes that occurred in the groundwater level near a polder road with a peat subgrade in the Netherlands after a relatively hot and dry summer. The draught problem became severe because of the presence of willows near the pavement edge. These types of trees are “heavy drinkers” and lowered the groundwater level even further resulting in excessive shrinkage and cracks in the pavement.

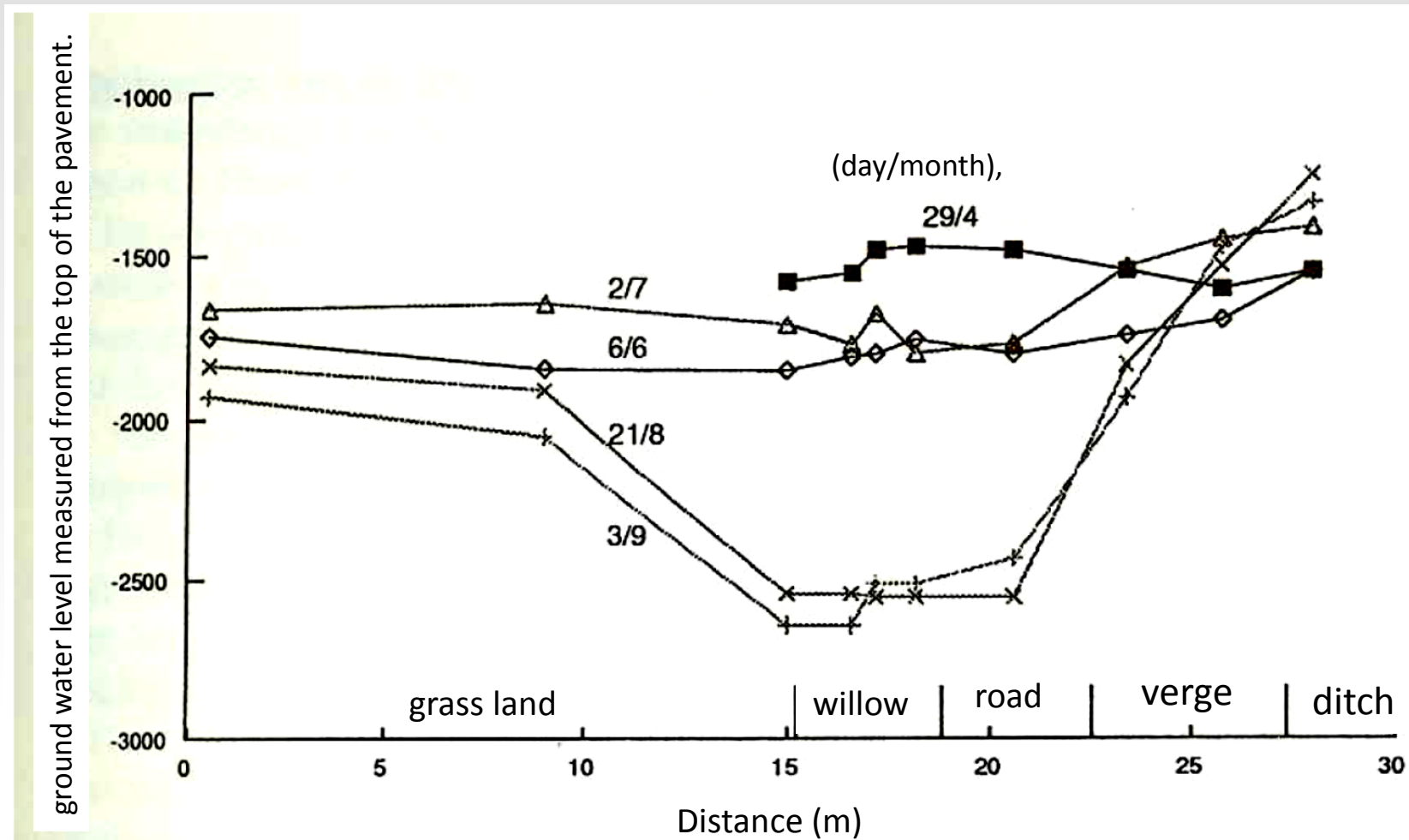


Figure 74: Changes in the transverse profile of a polder road due to shrinkage of the peat subgrade due to moisture loss in a hot and dry summer and the presence of poplars and willows.

Although it is clear that suction curves are extremely useful for the determination of moisture profiles, those curves are not readily available. Determination of soil suction in the laboratory is a time consuming test that has to be performed with great precision. If such curves are not available, soil suction of fine grained soils may be estimated by means of the equations given below which were reported by Saxton e.a. [29].

$$\psi = 100 A \theta^B$$

Where:

$\psi$  = water potential or matrix suction [kPa],

$\theta$  = volumetric moisture content [ $\text{m}^3 / \text{m}^3$ ],

$A = \exp [-4.396 - 0.0715 C - 4.880 * 10^{-4} S^2 - 4.285 * 10^{-5} S^2 C]$

$B = -3.140 - 0.00222 C^2 - 3.848 * 10^{-5} S^2 C$

$S$  = percentage sand being all particles between 2 mm and 50  $\mu\text{m}$ ,

$C$  = percentage clay being all particles smaller than 2  $\mu\text{m}$ .



Côté and Konrad presented an elegant procedure to estimate the hydraulic characteristics of unsaturated base-courses [30]. They used a schematized representation of the suction curve as shown in figure 75. The three most important parameters in this figure are  $\theta_s$  (saturated volumetric water content which is equal to the porosity of the soil  $n$ ),  $\psi_a$  (air entry value) and the slope of the curve  $\lambda$  (pore size distribution index). These parameters can be estimated using the following equations.

$$\log \psi_a = 3.92 - 5.19 n_f$$

Where:

$\psi_a$  = air entry value [kPa],

$n_f$  = porosity of the fine fraction =  $n / n_c$ ,

$n_c$  = porosity of the coarse fraction =  $n + (1 - n) F$ ,

$n$  = porosity of the entire skeleton including coarse and fine fraction =  $1 - \rho_d / \rho_s$ ,

$\rho_d$  = dry density [kg/m<sup>3</sup>],

$\rho_s$  = density of the particles [kg/m<sup>3</sup>],

$F$  = fines content (particles smaller than 50  $\mu\text{m}$ ) [%].

$$\lambda = 0.385 - 0.021 n_f^{0.65} S_{sf}$$

Where:

$S_{sf}$  = specific area of the fines fraction (to be determined in the laboratory) [m<sup>2</sup> / g].

Also the saturated hydraulic conductivity,  $k_s$ , can be estimated using:

$$\log (k_s * S_{sf}) = 9.94 n_f - 12.64 \quad [k_s] = [m / s]$$

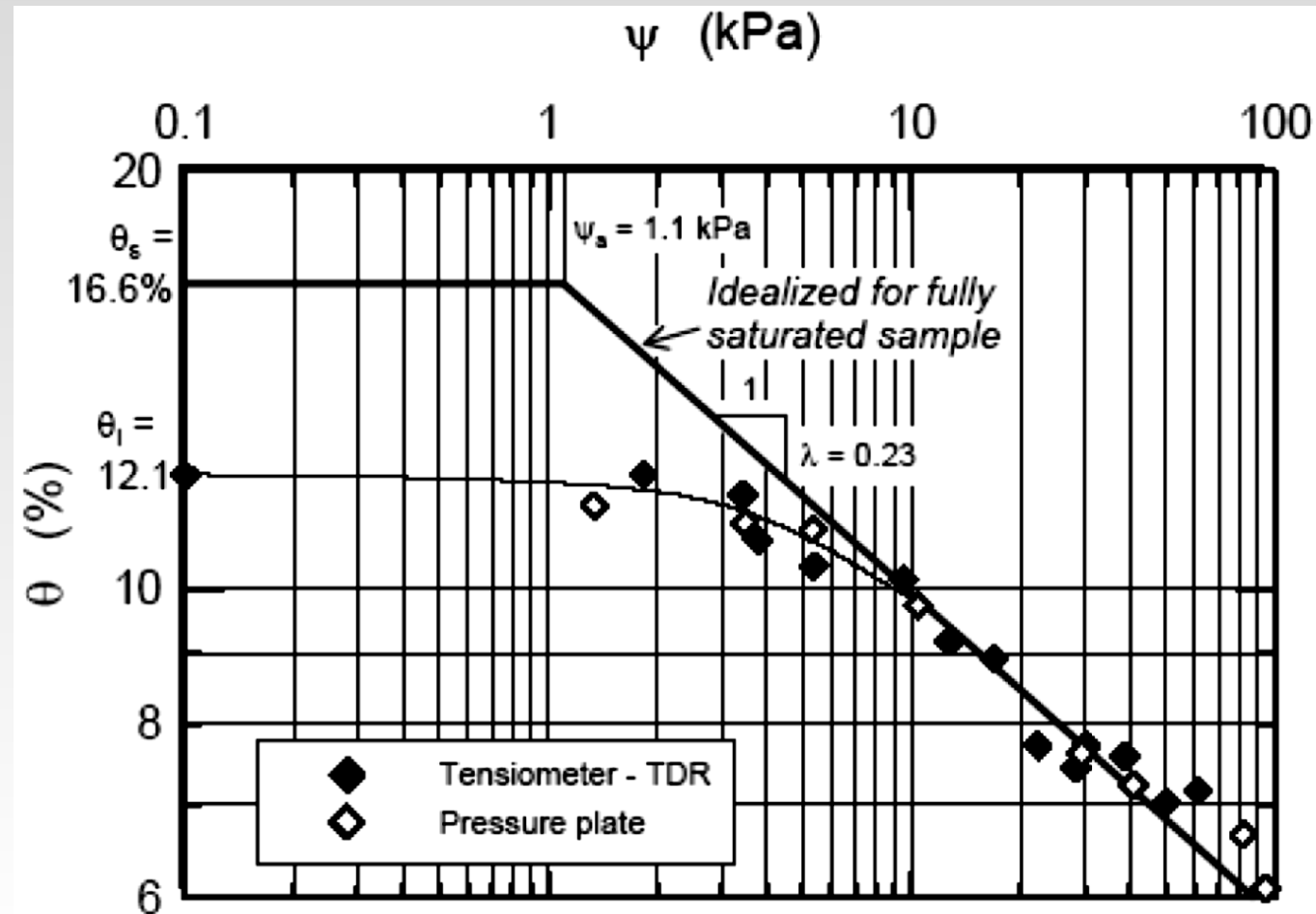
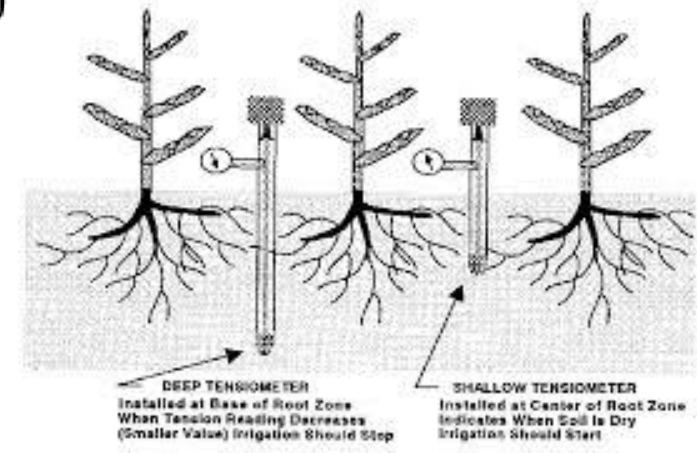


Figure 75: Idealized suction curve according to Côté and Konrad.



Although techniques are available to estimate the equilibrium moisture content using soil suction information, the equilibrium moisture content is also quite often estimated from regression equations developed from field observations. Examples of such equations are given hereafter.

Unbound subgrade:

$$\text{EMC} / \text{OMC} = 0.0084 \text{ LL}^{0.7} P_{0.425}^{0.3} + 0.34 \ln (100 + \text{Im}) + 0.11 P_{75} / \text{OMC} - 0.0036 P_{0.425} - 0.89$$

Non plastic subgrade:

$$\text{EMC} / \text{OMC} = 0.19 P_{75} / \text{OMC} + 0.0040 \text{ Im} - 0.0036 P_{0.425} + 0.53$$

Where :

EMC = equilibrium moisture content [%],

OMC = optimum moisture content determined by means of the modified Proctor test,

LL = liquid limit [%],

$P_{0.425}$  = percentage passing the 0.425 mm sieve,

$P_{75}$  = percentage passing the 75  $\mu\text{m}$  sieve,

Im = Thornthwaite moisture index.

$$I_m = (100 s - 60 d) / PET$$

Where:

s = maximum moisture surplus,

d = moisture deficit,

PET = potential evapotranspiration.

Typical values for Thornthwaite moisture index are given below.

Thornthwaite Index			Climate classification
	$I_m$	$>100$	peri-humid
$20 <$	$I_m$	$<100$	humid
$0 <$	$I_m$	$<20$	moist sub-humid
$-20 <$	$I_m$	$<0$	dry sub-humid
$-40 <$	$I_m$	$<-20$	semi-arid
	$I_m$	$<-40$	arid

It is suggested to use the unsoaked CBR values for subgrade design if  $EMC / OMC < 1.7$ .